archives
of thermodynamics
Vol. **40**(2019), No. 1, 85–102
DOI: 10.24425/ather.2019.128291

Optimization of absorption refrigeration systems by the method of computational experiment design

RIDHA BEN IFFA[a]
LAKDAR KAIROUANI[a]*
NAHLA BOUAZIZ[b]

[a] National Engineering School of Tunis

[b] University of Tunis El Manar

Abstract The objective of this work is to present an energy analysis of different absorption refrigerating systems operating with diverse refrigerants. Also is applied the method of experimental design to optimize configurations proposed by the absorption pairs used and the operating conditions. Both acceptable coefficient of performance and low operating generator temperature are scrutinised. Therefore, a computer program is developed. An investigation of the thermodynamic properties is presented. Results show the coefficient of performance evolution versus respectively the evaporator temperature, temperature of condensation and generator temperature. A particular interest is devoted to the intermediate pressure effect on the performance of different systems. In order to better converge in the selection of the configuration and the refrigerant, which can ensure a high coefficient of performance associated to relatively low operating generator temperature the plan of experiments has been developed, taking in account all parameters influencing the system performance and the function of operating temperature. Results show that the refrigerating machine containing a compressor between the evaporator and the absorber has a coefficient of performance quite acceptable and that it can work at low generator temperature for about 60 °C and using the $NH_3/LiNO_3$ as refrigerant.

Keywords: Absorption; COP; Evapo-compression; Refrigeration

*Corresponding Author. Email: lakdar_kairouani@yahoo.fr

Nomenclature

COP	–	coefficient of performance
C_P	–	specific heat at constant pressure, $Jkg^{-1}K^{-1}$
f	–	circulation ratio or driving factor
h	–	specific enthalpy, Jkg^{-1}
H_2O	–	water
LiBr	–	lithium bromide
$LiNO_3$	–	lithium nitrate
$\dot{m}$	–	mass flow rate, kgs^{-1}
NaSCN	–	sodium thiocyanate
NH_3	–	ammonia
P	–	pressure, Pa
$\dot{Q}$	–	heat transfer rate, W
S	–	entropy, $Jkg^{-1}K^{-1}$
T	–	temperature, °C, K
W	–	mechanical power, W
x	–	mass fraction, %

Greek symbols

γ	–	isentropic coefficient
ε	–	cooling efficacy

Subscripts

1	–	first stage
2	–	second stage
AB	–	absorber
CD	–	condenser
COM	–	compressor
ECH	–	inter-exchanger solution
Ent	–	input
EV	–	evaporator
FF	–	refrigerant
GE	–	generator
L	–	liquid
in	–	inlet
out	–	outlet
p	–	weak solution
r	–	rich solution
v	–	vapor

1 Introduction

Absorption machines have several advantages such as protecting the environment and the nature. Additionally this type of refrigerating machines does not use CFCs fluids (chlorofluorocarbons), which deplete the ozone layer, Kang *et al.*[1], Boer *et al.* [2], Göktun [3], Laouir *et al.* [4]. Besides they are quiet compared to vapor compression machines, Riffat and Guoquan [5].

There are several models of absorption machines, as a simple stage machines consisting of an absorber, evaporator, condenser and a generator, which are conventional absorption machines. Such machine is working between two pressure levels (P_{EV} – evaporator pressure and P_{CD} – condenser pressure); it has been the subject of several studies, Alvares and Trepp [6], Misra *et al.* [7], Mumah *et al.* [8], Kouremenos [9], Hulten and Berntsson [10], Göktun [11], and G. Sachdeva *et al.* [12].

Other models composed of different stages with different associations between the system components; they worked at three pressure levels, Saghiruddin and Siddiqui [13], Bouaziz *et al.* [14–15], Charia *et al.* [16] and Kumar [17]. There is a wide range of refrigerant couples that can be used for the refrigerating machine such us NH_3/H_2O, NH_3/NaSCN and $NH_3/LiNO_3$, Rodakis and Antonopoulos [18], Linghui Zhu and Junjie Gu [19], Kairouani *et al.* [20], and S. Anand *et al.* [21].

The cooling demand in summer, in hot climate countries, leads to a peak in electricity consumption, the use of alternative technologies should be favored. One possibility consists in the solar absorption refrigerating systems, Tarsitano *et al.* [22], Petela *et al.* [23] and Alobaid *et al.* [24]. Their principal advantages compared to mechanically driven compression cycles are the use of natural refrigerants, but their coefficient of performance (COP) values are relatively low compared to vapor compression refrigerators. The experimental and theoretical works on absorption systems are quite numerous, Yi Chen *et al.* [25] and Corey *et al.* [26].

In this study, four absorption system configurations and four couples refrigerant/absorbent were considered. The evaporation, condensation and generator temperatures were varied. The method of design of experiments is used to identify optimal situations and particularly the configuration that works with low generator temperatures.

2 Description and analysis of the systems

2.1 Description of the systems

A single effect absorption refrigeration cycle, for which details are provided elsewhere, Bouaziz *et al.* [27], is shown in Fig. 1. The cascade cycle (cascade 1) and double stage cycle (cascade 2) represented respec-

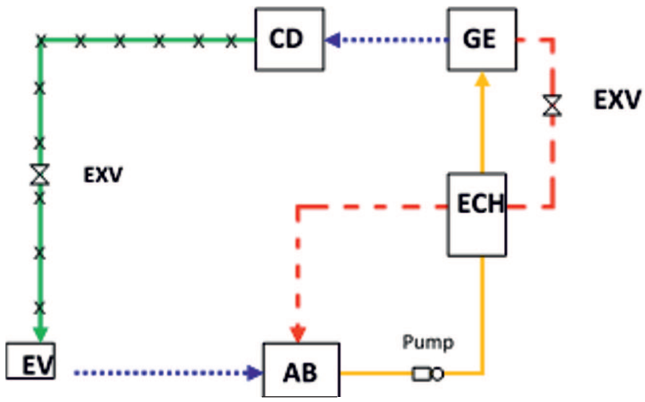

Figure 1: Single effect absorption refrigeration system: AB – absorber , CD – condenser, COMP – compressor, EV – evaporator, ECH – heat exchanger, EXV – expansion valve, GE – electric generator.

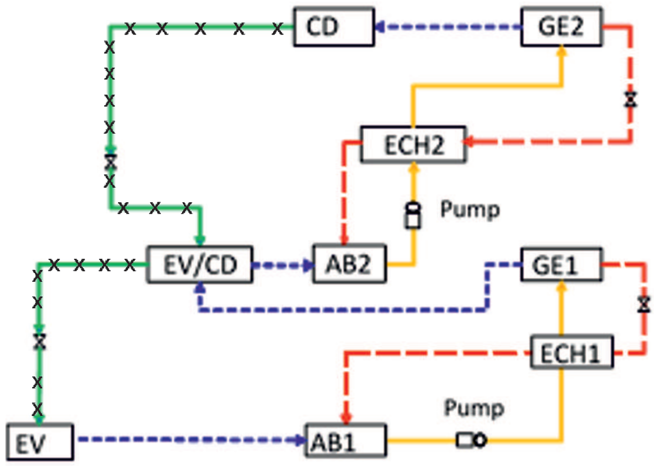

Figure 2: Cascade 1.

tively in Figs. 2 and 3 are developed by Bouaziz *et al.* [14,15,27]. The new cycle evaporator-compressor-absorber (ECA) is composed by an evaporator, absorber, generator, condenser and a compressor inserted between the evaporator and the absorber. The cycle is represented in Fig. 4.

Three pressure levels are present in the ECA configuration: the generator and condenser operate at high pressure whereas the evaporator at

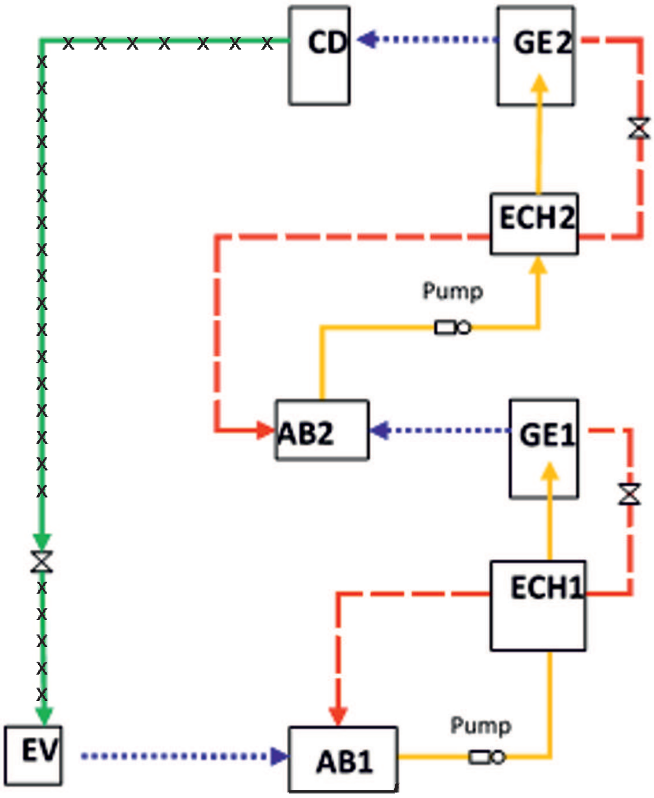

Figure 3: Cascade 2.

low pressure, while the absorber operates at an intermediate pressure. The refrigerant (NH_3 for NH_3/H_2O, NH_3/NaSCN, $NH_3/LiNO_3$ and H_2O for H_2O/LiBr) vapor leaves the generator (GE) and enters in the condenser (CD). The weak solution (dashed line) exiting the generator passes through the solution heat exchanger (ECH) before entering in the absorber (AB); the refrigerant condensate (solid line with cross symbols) passes through expansion valve (EXV) and enters the evaporator (EV), where it vaporizes, producing a cooling effect. Vapor (dotted line) exiting the compressor (COMP) enriches the solution in the absorber. The strong solution (solid line) exiting the absorber passes through the solution heat exchanger and enters to the generator.

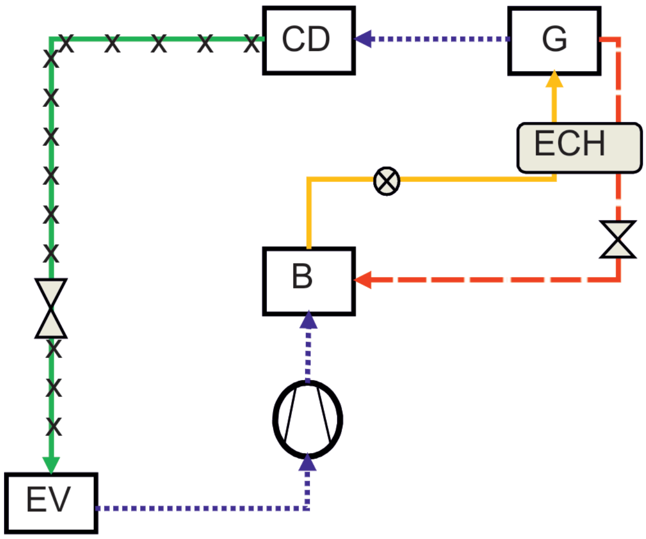

Figure 4: Cycle of evapo-compression (ECA).

2.2 Energy and mass balances

The mass balance governing the three present substances: weak solution, rich solution, and refrigerant gas gives

$$\dot{m}_{FF} + \dot{m}_p - \dot{m}_r = 0 \ . \tag{1}$$

The mass balance for refrigerant gives:

$$\dot{m}_{FF} + x_p \dot{m}_p - x_r \dot{m}_r = 0 \ . \tag{2}$$

The specific solution circulation factor *f*, which represents the mass of rich solution per one kilogram of vapor refrigerant leaving the generator, is given by

$$f = \frac{(1 - x_p)}{(x_r - x_p)} \ . \tag{3}$$

The rich and weak solution flow rates are given by:

$$\dot{m}_r = \dot{m}_{FF} f \ , \tag{4}$$

$$\dot{m}_p = \dot{m}_{FF}(f - 1) \ . \tag{5}$$

Energy balance for each installation component is presented by the following general equations:

$$\dot{Q}_{CD} = \dot{m}_{FF}(h_v - h_{out}) \ , \tag{6}$$

$$\dot{Q}_{AB} = \dot{m}_{FF}\left[h_v + (f-1)h_{in} - f h_{out}\right] \ , \tag{7}$$

$$\dot{Q}_{GE} = \dot{m}_{FF}\left[h_v + (f-1)\,h_{out} - f h_{in}\right] \ , \tag{8}$$

$$\dot{Q}_{EV} = \dot{m}_{FF}(h_v - h_{in}) \ . \tag{9}$$

The value of enthalpy h_v, h_{in}, and h_{out} are not the same for all components.

For an isentropic process, the Laplace relation gives

$$T_{in}P_{\ in}{}^{(1-\gamma)/\gamma} = T_{out}P_{out}{}^{(1-\gamma)/\gamma} \ , \tag{10}$$

where T_{in}, P_{in} and T_{out}, P_{out} are the compressor temperature and pressure at inlet and outlet, respectively.

Under the assumption of isentropic processes (ideal case), the consumed power is given by

$$W_{is} = \dot{m}_{FF}C_P(\ T_{out} - T_{in}) \ . \tag{11}$$

Taking into account of the isentropic efficiency, η_{is}, the real power is given by

$$W_{real} = \frac{W_{is}}{\eta_{is}} \ , \tag{12}$$

$$W_{is} = \dot{m}_{FF}(h_{out} - h_{in}) \ , \tag{13}$$

were the isentropic efficiency is given by Brunin *et al.* [28]

$$\eta_{is} = 0.874 - 0.0135\tau \tag{14}$$

with

$$\tau = \frac{P_{AB}}{P_{EV}} \ , \tag{15}$$

where P_{AB} and P_{EV} are the absorber and evaporator pressure levels, respectively. The coefficient of performance is given by the following expression:

$$\text{COP} = \frac{Q_{EV}}{Q_{GE} + W_{Pump}} \ . \tag{16}$$

The cooling efficacy is given by the following expression:

$$\varepsilon = \frac{Q_{EV}}{Q_{GE} + W_{COM}} \ . \tag{16'}$$

The cooling efficacy is defined for the evapo-compression system (ECA) only.

3 General assumptions

- All components are in steady state conditions.
- No imperfections in both generator and absorber.
- Pressure drops are negligible in all conducts.
- At the generator exit, the refrigerant vapor is pure.
- The effectiveness of the solution heat exchanger is 80% [29].
- Pump consumption is negligible.

4 Results and discussion

Several studies have been devoted to determine the cooling efficacy or coefficient of performance and limitations of absorption system operating conditions, Laouir *et al.* [4]. In order to evaluate the refrigeration absorption system performance, relative to different previously presented configuration, a numerical program was developed. The calculating procedures of the fluid thermodynamic properties and the performance coefficient were obtained using the Maple computer tools. The numerical simulation, developed in the present investigation carries out a comparative study of the reference system performances.

4.1 Performances of the simple stage

Figure 5 shows the cooling efficacy's evolution versus the generator temperature, for an evaporator temperature and a condenser temperature fixed respectively to 10 °C and 40 °C. The H_2O/LiBr couple gives the maximum COP for a generator temperature higher than 75 °C.

4.2 Performances of the cascade 1 system

The temperature of the evapo-condenser is fixed at 25 °C. Figure 6 shows the COP evolution versus the temperature of the generator (the operating temperature) for different fluids, with $T_{EV} = 10$ °C and $T_{CD} = 40$ °C. The H_2O/LiBr couple gives the maximum COP for a generator temperature below 60 °C.

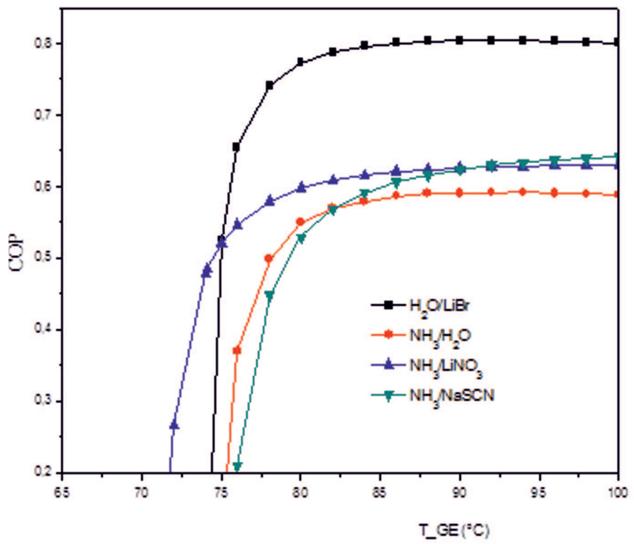

Figure 5: COP of the simple stage system evolution versus T_{GE} with $T_{EV} = 10\,^{\circ}$C, and $T_{CD} = 40\,^{\circ}$C.

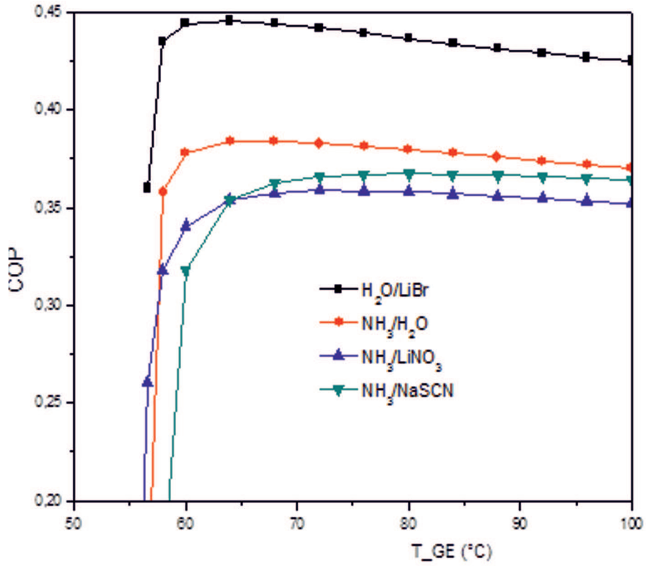

Figure 6: COP of the cascade 1 system evolution versus T_{GE} with $T_{EV} = 10\,^{\circ}$C, and $T_{CD} = 40\,^{\circ}$C.

4.3 Performances of the cascade 2 system

Figure 7 shows that the operating temperature is relatively lower than for the classic system. It is less than 70 °C for all fluids, where T_{EV}, T_{CD}, and P_{int} are fixed respectively at 10 °C, 40 °C and 3 kPa for H_2O/LiBr and 750 kPa for the other fluids. The H_2O/LiBr couple gives the maximum COP for a generator temperature below 60 °C.

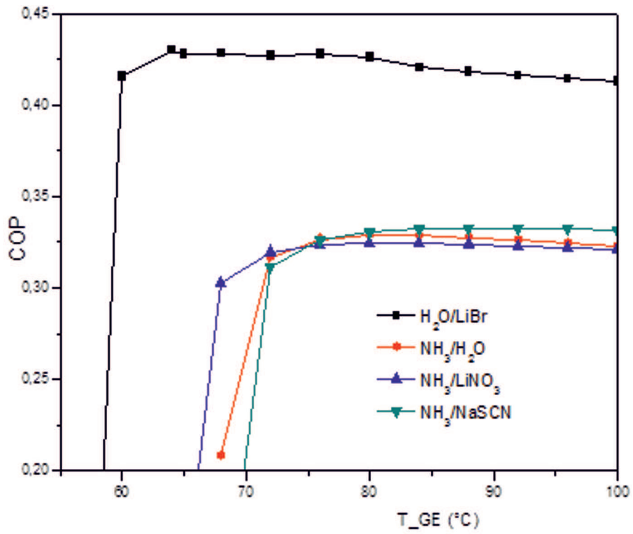

Figure 7: COP of the cascade 2 system as a function of a T_{GE} with $T_{EV} = 10$ °C and $T_{CD} = 40$ °C.

4.4 Performances of the new cycle

In the new cycle, the evaporator temperature and condenser temperature for each family of curves are fixed. The numerical results illustrate the evolution of the cooling efficacy for different generator temperatures, Fig. 8.

Figures 5–8 show that the H_2O/LiBr is a performing fluid, but the operating temperature is higher relative to other fluids. The cascade cycles decrease operating temperatures in the generator but they have a low COP. The novel configuration has the double advantages of single stage (high cooling efficacy) and cascade cycle which operates at low temperature.

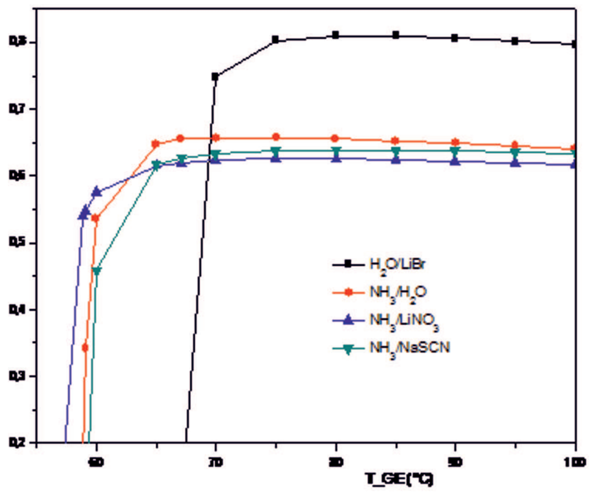

Figure 8: Cooling efficacy (ε) of the novel system as a function of a T_{GE} with T_{EV} = 10 °C and T_{CD} = 40 °C.

Following the large number of results, the experiment design methodto determine the right combination is used.

5 Experiment design

The objective of this research is to maximize the COP or the cooling efficacy by maintaining a minimal value of the operating temperature (T_{GE}). It should be noted that the COP and the cooling efficacy depend on three basic parameters:

- generator temperature (T_{GE}),
- evaporator temperature (T_{EV}),
- condenser temperature (T_{CD}).

The pair/couple used in the study and the installation type affect the COP and the cooling efficacy. For a minimal value of T_{CD} or T_{GE} or a maximal value of T_{EV}, the COP and the cooling efficacy are optimal. In our investigation 5 factors with 4 levels are done (see Tab. 1).

There are two types of experimental plans: factorial, which require a high number of experiments (in our case, for example, five factors of four

Table 1: Factor and levels.

Factor	Levels	Factor	Levels, °C	Factor	Levels, °C
Cycle	N cycle Casc 1 Casc 2 Simple	T_{EV}	5 10 15 20	T_{GE}	65 75 85 100
Fluid	H_2O $LiNO_3$ NaSCN LiBr	T_{CD}	25 30 35 40		

Table 2: The experiment design.

Cycle	Absorbent	T_{EV}, °C	T_{CD}, °C	T_{GE}, °C	COP, or ε
N Cycle	H_2O	10	30	65	0.71
N Cycle	$LiNO_3$	15	35	75	0.68
N Cycle	NaSCN	20	40	85	0.69
N Cycle	LiBr	25	45	100	0.84
Cascade 1	H_2O	15	40	100	0.38
Cascade 1	$LiNO_3$	10	45	85	0.35
Cascade 1	NaSCN	25	30	75	0.39
Cascade 1	LiBr	20	35	65	0.47
Cascade 2	H_2O	20	45	75	0.45
Cascade 2	$LiNO_3$	25	40	65	0.46
Cascade 2	NaSCN	10	35	100	0.35
Cascade 2	LiBr	15	30	85	0.34
Simple	H_2O	25	35	85	0.73
Simple	$LiNO_3$	20	30	100	0.71
Simple	NaSCN	15	45	65	0.00
Simple	LiBr	10	40	75	0.52

levels give $4^5 = 1024$ experiments) and fractional plans which can reduce the number. In this study, a Carré Hyper Greco-Latin plan consisting of

16 experiments is used. The possible combinations are drawn in Tab. 2.

From Fig. 9, it is deduced that all the factors have a significant effect, and to obtain an acceptable COP or cooling efficacy with low temperature of the generator, the evapo-compression cycle can be used.

The five factors are represented with their levels and their influence on the performance of an absorption machine in Fig. 9. The most influential factor on the COP or cooling efficacy is the type of refrigeration cycle. Other factors have almost the same effect on the value of the COP or cooling efficacy.

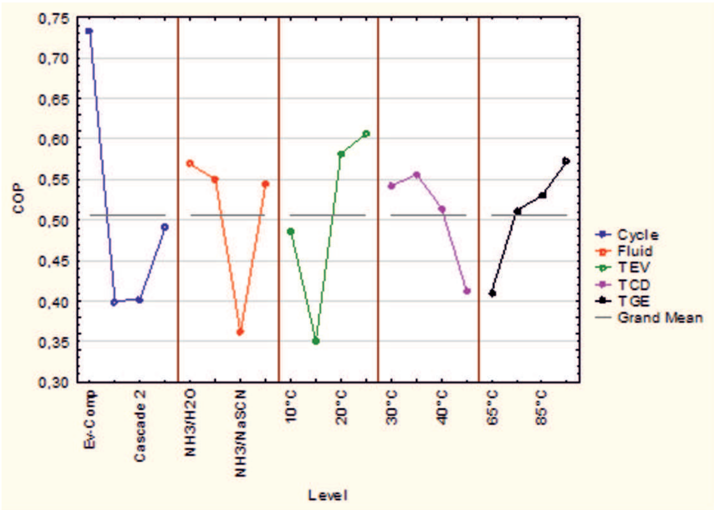

Figure 9: Graph of main effects

In order to make the results more legible, a three-dimensional representation was used. In Figs. 11 to 12, the optimal COP or cooling efficacy is plotted against T_{GE}, T_{CD}, and T_{EV} for all four cycles. In Fig. 13, the optimal COP is shown as a function of the nature of the refrigerant couple for the four cycles.

Figures 10 and 11 confirm that the new cycle can operate in difficult conditions on the level of the condenser (high T_{CD}) with low temperatures of the generator while the classical machine cannot operate unless the temperature is above 75 °C and condensing temperature lower than 40 °C to provide the same COP or cooling efficacy than the new installation for $T_{GE} = 65\,°C$ and $T_{CD} = 45\,°C$.

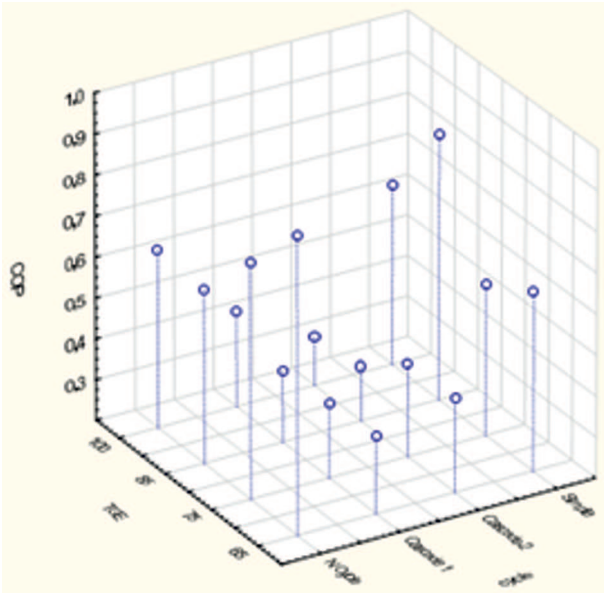

Figure 10: COP or cooling efficacy versus T_{GE} and type of cycle.

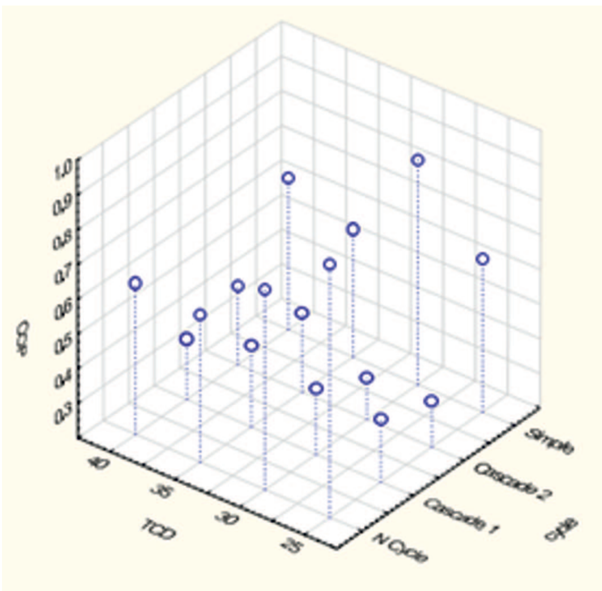

Figure 11: COP or cooling efficacy versus T_{CD} and type of cycle.

The iso-responses of Fig. 12, show that evapo-compression system (ECA) works for an evaporation temperature range wider than other systems. It gives acceptable cooling efficacy values between 0.7 and 0.9 at relatively low temperatures at the evaporator.

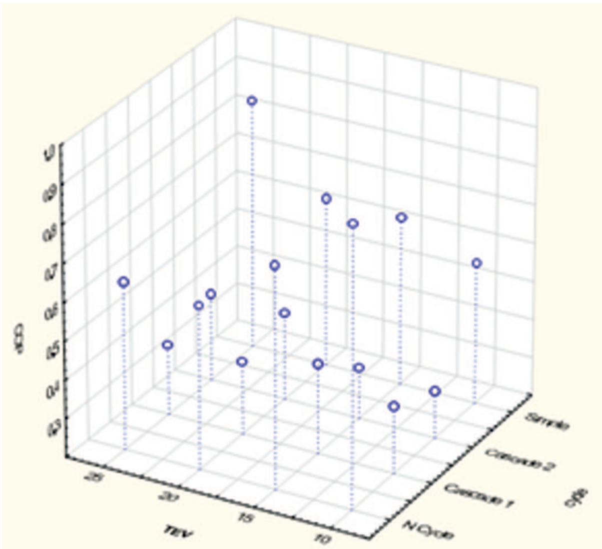

Figure 12: COP or cooling efficacy versus T_{EV} and type of cycle.

Figure 13 shows that the performance and optimum coefficient for the evapo-compression machine (ECA) are obtained for the four pairs used. The single stage has the highly efficient only for classic couples NH_3/H_2O and H_2O/LiBr. Cascading cycles remain non-performing; their COP does not exceed 0.5 in the best operating conditions.

6 Conclusions

The conventional machine provides a coefficient of performance considered as acceptable. It operates with an operating generator temperature around 75 °C for a condensation temperature of 40 °C and an evaporation temperature of 10 °C.

The cascade cycles 1 and 2 operate with a low generator temperature but their coefficient of performance is half of the simple machine. They have an operating problem in the first and second levels and this is due to the difference between the titles of the rich and the poor solution which is

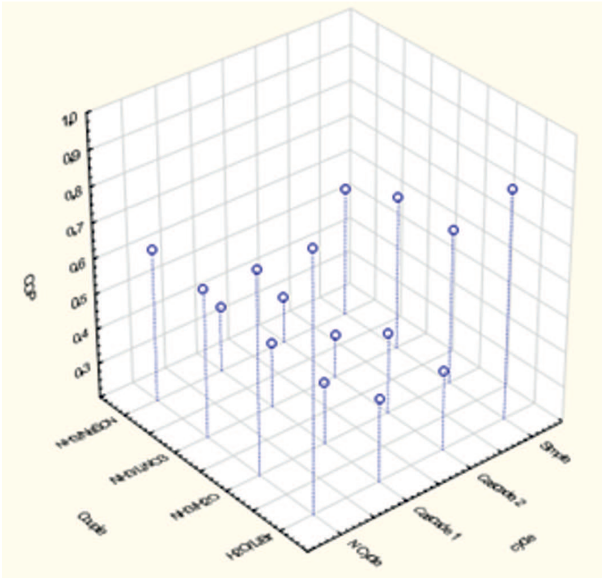

Figure 13: COP or cooling efficacy versus fluid nature and type of cycle.

very low. Therefore the driving factor, *f*, is very large and the generator heat consumption increases.

The new configuration has a cooling efficacy higher than the cascade cycles and the simple machine. Besides, it operates with a generator temperature lower than the cascade cycles. The new configuration can operate for generator temperature less than 60 °C for NH_3/H_2O, NH_3/NaSCN and $NH_3/LiNO_3$ with the same temperatures of the evaporator and condenser. If low temperature heat energy is free (recovery of exhaust gases, solar energy, geothermal energy, etc.), the coefficient of performance of the new system would be quite high and the system would be profitable.

Received 21 August, 2017

References

[1] Kang Y.T., Kunugi Y., Kashiwagi T.: *Review of advanced absorption cycles: Performance improvement and temperature lift enhancement.* Int. J. Refrig. **23**(2000), 388–401.

[2] Boer D., Valles M., Coronas A.: *Performance of double effect absorption compression cycles for air–conditioning using methanol–TEGDME and TFE–TEGDME*

systems as working pairs. Int J. Refrig. **21**(1998), 542–555.

[3] Göktun S.: *Performance analysis of a heat engine driven combined vapor compression-absorption-ejector refrigerator.* En. Con. Mgmt. **41**(2000), 1885–1895.

[4] Laouir A., Legoff P., Hornt J.M.: *Cycle de frigopompes ŕ absorption en cascades matérielles–détermination du nombre d'étages optimal pour le mélange ammoniac–eau.* Int J. Refrig. **25**(2002), 136–148.

[5] Riffat S.B., Qiu G.: *Comparative investigation of thermoelectric air-conditioners versus vapour compression and absorption air-conditioners.* App. Th. Eng. **24**(2004), 1979–1993.

[6] Alvares S.G., Trepp Ch.: *Simulation of solar driven aqua-ammonia absorption refrigeration system.* Int. J. Refrig. **10**(1987), 40-49.

[7] Misra R.D., Sahoo P.K., Gupta A.: *Application of the exergetic cost theory to the LiBr/H_2O vapour absorption system.* Energy **27**(2002), 1009–1025.

[8] Mumah S.N., Adefila S.S. and Arinze E.A.: *First law thermodynamic evaluation and simulation of ammonia-water absorption heat pump systems.* En. con. Mgmt. **35**(1994), 737–750.

[9] Kouremenos D.A.: *A tutorial on reversed NH_3/H_2O absorption cycles for applications.* Solar Energy **34**(1985), 101–115.

[10] Hulten M., Berntsson T.: *The compression/ absorption heat pump cycle-conceptual design improvements and comparisons with the compression cycle.* Int. J. Refrig. **25**(2002), 487–497.

[11] Göktun S.: *Optimal performance of an irreversible, heat engine-driven combined vapour compression and absorption refrigerator.* App. Energy **62**(1999), 67–79.

[12] Sachdeva G., Jain V., Kachhwaha S.S.: *Energy Analysis of a vapor compression system cascaded with ammonia-water absorption.* Int. J. Air-Cond. Refrig. **22**(2014) doi:10.1142/S2010132514500072

[13] Saghiruddin, Siddiqui M.A.: *Economic analysis of two stage dual fluid absorption cycle for Optimizing generator temperatures.* En. Con. Mgmt. **42**(2001), 407–437.

[14] Bouaziz N., Ben Iffa R., Kairouani L.: *Performance of a water ammonia absorption system operating at three pressure levels.* J.M.E.R. **3**(2011), 120–127.

[15] Bouaziz N., Ben Iffa R., Kairouani L.: *Avantage d'une configuration de machine á absorption operant á trois niveaux de pression.* Mécaniq. Ind. **12**(2011), 103–107.

[16] Charia M., Pilatte A., Bouidida M.: *Machine frigorifique ŕ absorption (eau-ammoniac) fonctionnant avec des capteurs plans sur le site de Rabat.* Rev. Int. Froid **14**(1991), 297–303.

[17] Kumar S.: *Experimental studies of a three-pressure absorption refrigeration cycle.* Rev. Int. Froid **16** (1993), 31–39.

[18] Rodakis E.D., Antonopoulos K.A.: *Thermodynamic cycle, correlations and nomograph for NH_3-NaSCN absorption refrigeration systems.* H. R. Syst. CHP **15**(1995), 591–599.

[19] Zhu L., Gu J.: *Second law-based thermodynamic analysis of ammonia/sodium Thiocyanate absorption system*. Renew. Energ. **35**(2010), 1940–1946.

[20] Kairouani L., Nahdi E., Iffa R.B.: *Thermodynamic investigation of tow stage absorption refrigeration system connected by a compressor*. Am. J. App. Sc. **2**(2005), 1036–1041.

[21] Anand S., Gupta A., Tyagi S.K.: *Exergy analysis of a LiBr–H_2O vapor absorption refrigeration plant: A case study*. Int. J. Air-Cond. Refrig. **22**(2014), doi: 10.1142/S2010132514500102.

[22] Tarsitano A., Ciancio V., Coppi M.: *Air-conditioning in residential buildings through absorption systems powered by solar collectors*. En. Proc. **126**(2017), 147–154.

[23] Petela K., Manfrida G., Szlek A.: *Advantages of variable driving temperature in solar absorption chiller*. Ren. En. 114B (2017), 716–724.

[24] Alobaid M., Hughes B., Calautit J.K., O'Connor D., Heyes A.: *A review of solar driven absorption cooling with photovoltaic thermal systems*. Ren. Sus. En. Rev. **76**(2017), 728–742.

[25] Chen Y., Han W., Jin H.: *Thermodynamic performance optimization of the absorption-generation process in an absorption refrigeration cycle*. En. Con. Mgmt. **126**(2016), 290–301.

[26] Misenheimer C.T., Terry S.D.: *The development of a dynamic single effect, lithium bromide absorption chiller model with enhanced generator fidelity*. En. Con. and Mgmt. **150**(2017), 574–587.

[27] Bouaziz N., Iffa R.B., Nehdi E., Kairouani L.: *Conception of an absorption refrigerating system operating at low enthalpy sources*. Thermodynamics systems in equilibrium and non equilibrium; ISBN: 978-953-307-283-8, InTech. (2011).

[28] Brunin O., Feidt M., Hivet B.: *Comparison of the working domains of some compression heat pumps and a compression-absorption heat pump*. Int J. Refrig. **20**(1997), 5, 308–318.

[29] Sun D.W.: *Comparison of the performances of NH_3-H_20, NH_3-$LiNO_3$ and NH_3-NaSCN absorption refrigeration systems*. En. Con. Mgmt. **39**(1998), 5-6, 357–368.